1 Introduction

> "A very satisfactory explanation of the physical process in the boundary layer between a fluid and a solid body could be obtained by the hypothesis of an adhesion of the fluid to the walls, that is, by the hypothesis of a zero relative velocity between fluid and wall. If the viscosity was very small and the fluid path along the wall not too long, the fluid's velocity ought to resume its normal value at a very short distance from the wall. In the thin transition layer, however, the sharp changes of velocity, even with small coefficient of friction, produce marked results."
>
> - Ludwig Prandtl (1904) – Address to the 3rd Mathematical Congress in Heidelberg

1.1 Motivation

Our understanding of TBL over flat plate related to its function in flight, heat convection in turbines or regarding propellers, hydrodynamics and several other similar engineering applications had been immensely investigated during last century and has continues till today. In a more general sense the wall-bounded turbulent flows are of special importance due to their scientific relevance and also their technical applications. Therefore, they have been regarded as an important topic for physicists, mathematicians and engineers, inspiring wide ranges of studies. The intrigue boundary conditions imposed by the wall bounded turbulent flows in terms of the structures and their scales in the process of transport and dissipation of the turbulent kinetic energy, plays a vital role determining associated friction drag. On the other hand, skin friction drag as a function of total drag, is of keen interest in terms of practical applications.

Flow Control Technique's for turbulent boundary layer has an wide engineering application from modern aircraft to the high speed trains and cars. Estimations show that, nearly 50% of the total drag of an subsonic aircraft and 30% from automobiles are constituted from skin friction drag (Kornilov (2005)). Airline and truck industry consumes 238.5 billion and 190 billion litres of oil per year respectively, out of which 25% and 27% fuel is spent to overcome the viscous drag (Wood (2004)). In United States alone, 40% drag is coming from skin friction in transportation sector whereas for a subsonic long range passenger liner, approximately 50% of the total drag is contributed from friction, 70% for marine vessels and ~100% for long pipeline pumping (Wood (2004)). Only 1% of reduction of such skin friction drag can save upto 400,000 litres of fuel yearly (based on Airbus A320 aircraft data (Kim et al. (2011))).

Large part of the fuselage, wing, tail wing and radar section of a subsonic aircraft has the potential to deploy drag reduction mechanisms. Due to their size and operating speeds, the majority of commercial and military aircraft in service today are dominated by flows that results from the presence of turbulent boundary layer. This generally cover the most of the aircraft's surface. It is well known that turbulent boundary layer significantly increases the skin friction drag penalties when compared to laminar boundary layers. Moreover, they do result in a reduced susceptibility to flow separation due to their robustness to surface imperfections. Therefore, turbulent drag reduction has a direct relationship to the eddy structures of different size and scales present in the boundary layer.

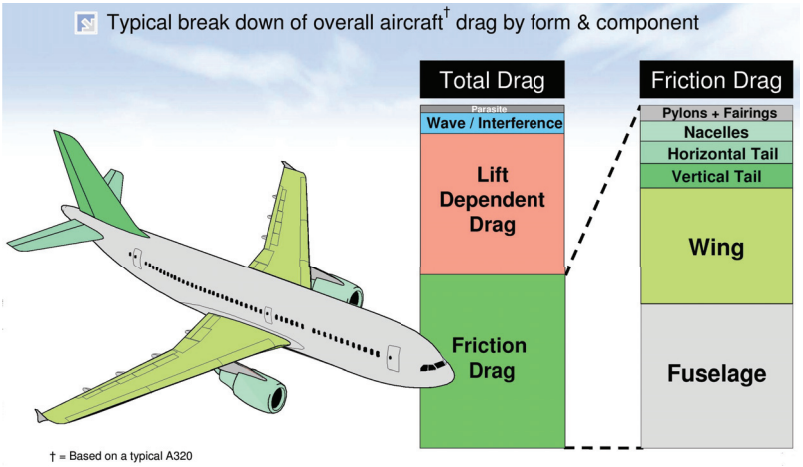

Figure 1.1: Break down of the drag contribution according to the drag types on different aircraft component (Hills (2008)).

Form/Pressure drag contribution to an aerodynamic body can be minimized with an optimized and streamlined design where as skin friction drag being the largest contributor than the former one. Apart from advances in designing streamlined body for aircraft, reduction of friction drag is the only possibility to improve aerodynamic efficiency (Kim et al. (2011)).

Figure-1.1 exhibit the contribution of different types of drag on a subsonic A320 aircraft according to its surface sections. This indicates that nearly half of the total drag comes from the friction drag. For aero and thermodynamic applications, flow control based on the varying surface conditions has been and still, of keen interest where motivation is focused towards the drag reduction, which in turn, can lead to significant financial benefit.

1.2 Turbulent flows

Most of the flows we encounter in nature as well as engineering applications are turbulent. It is both spatial and temporal instability and swirling of different scales caused by a continuous mixture of complex flows. A turbulent flow may arise due to the effect of frictional force on the surface of a stationary wall being flowed around or due to the interaction between flows at different rates. Moreover, a turbulent flow is characterized by the fact that its velocity and pressure in a spatial reference point are unstable over time. Particularly for wall bounded turbulent flows, the bounding energy content between the free stream flow and the underlying surface fluctuate depending on the flow Reynolds number and viscous effect. This type of instability with continuous change of state means that a turbulent flow can only be characterized by a series of parameters. These parameters include:

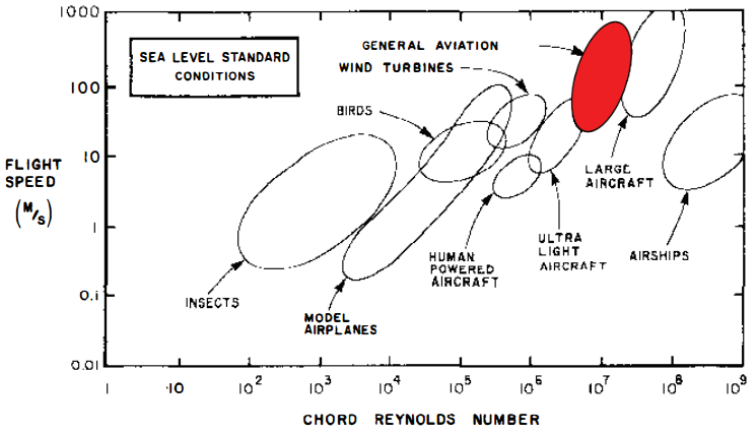

Figure 1.2: Operating range of different flying objects where red oval indicate the ranges for the general aviation (Lissaman (1983)).

1. Unsteadyness: A turbulent flow is irregular, disordered or chaotic and random. Despite chaotic behavior, the turbulence is de-terminus and can be described by the Navier-Stokes equations. Many probabilistic turbulence models allow to determine the most important parameters of the turbulent flow such as speed, temperature and pressure.

2. Diffusion: Increase in diffusion also causes an increase of the wall shear stress in the near wall region and results in an increase of the frictional resistance.

3. Dissipation: The kinetic energy of the flow is very quickly converted into internal energy of the small vortex or turbulence scales.

4. Three-dimensionality: The turbulent flow is always three-dimensional. It means that only in the case of averaged equations over time one can consider the turbulent flow as partially two-dimensional. In reality, none of the components of flow velocity ever equals zero. However, we assume two-dimensionality for simplification.

5. Continuity: Change of the turbulence parameters is a continuous process. In turbulent flows, some processes increase and other processes weaken simultaneously.

6. High Reynolds number: A turbulent flow appears above a specific Reynolds number range.

From the previous discussion, we now know that TBL gives rise to the skin friction comparatively higher than the laminar ones. This is due to the fact that at sufficiently high Reynolds number the boundary layer flow becomes turbulent shortly after the leading edge. Therefore, large part of the wall encounters turbulence and its associated skin friction drag. Most of the subsonic passenger airliners are operated at the high Reynolds number, where most of the aerodynamic surfaces of fuselage, wings and different control surfaces are subjected to high Reynolds number. Figure-1.2 shows the operating range of the subsonic passenger airliners where vertical and lateral axis presents the operating velocity and their corresponding chord Reynolds number (Re_C) respectively. Here, $Re_C \geq 10^6$ is the regime where most of the general aviation operations are performed.

1.3 Turbulent Boundary Layer

Under certain conditions, such as at large Reynolds numbers laminar flow becomes unstable and eventually, turn into turbulent. To explain this phenomenon, one can theoretically explain as follows. The small perturbations overlap at the beginning of the laminar flow. As these perturbations grow with the Reynolds number, eventually the boundary layer changes into an unstable one due to increasing perturbation and finally, transforms into the turbulent form.

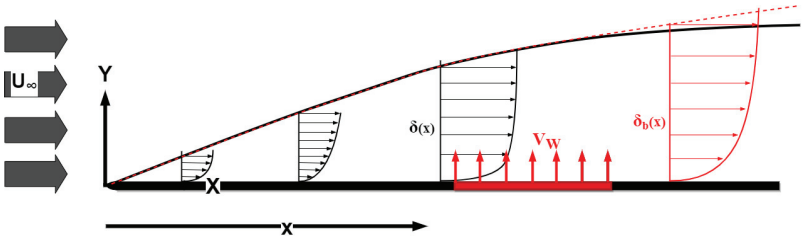

Figure 1.3: turbulent boundary layer developing on a flat plate with wall-normal transpiration from localized perforated surface (not scaled).

In order to distinguish between the classical turbulent boundary layer over non permeable surface and blowing boundary layer with perforated wall, reference turbulent boundary layer over a smooth wall will be referred as $_{SBL}$. A schematic of boundary layer developed over a flat plate is presented in Figure-1.3, where a perforated surface replaces the non permeable one in the red region where velocity magnitude of wall normal blowing is indicated with V_W.

The origin of the Cartesian co-ordinate system for presented one started at the leading edge of the flat plate, however, the ideal model of a turbulent boundary layer develops over a flat plate that is infinitely long along streamwise and spanwise direction. The ideal flat plate geometry which we refer to fulfills the zero pressure gradient condition, therefore, free stream velocity outside the boundary layer is given by U_∞.

Here, boundary layer thickness (BLT) over Standard Boundary Layer (SBL) and blowing boundary layer is indicated with a solid black line and dashed red line respectively. They are termed as $\delta(x)$ and $\delta_b(x)$ respectively as a function of streamwise distance from the leading edge. Previous literature survey suggested that the Micro-blowing Technique gives rise to boundary layer thickness depending on the magnitude of the blowing velocity. Figure-1.3 exhibit the growth of the boundary layer (not scaled) with the dashed line when blowing is applied. Based on the hypothesis that boundary layer thickness is gradually increased due to blowing therefore, boundary layer thickness (δ_b) is larger than the ones from Standard Boundary Layer e.g $\delta(x) < \delta_b(x)$.

1.4 Problem statement

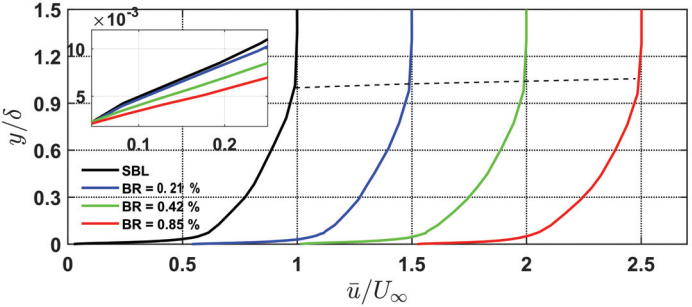

Figure 1.4: Profiles of a streamwise velocity profile scaled with the outer scaling parameter with different BR including reference Standard Boundary Layer at $Re_{\theta,SBL}$ = 1870. Profiles are offset from each other along x axis by 0.5. Black "dashed" line indicate the points connecting the edge of boundary layer where mean streamwise velocity reaches 99% of the free stream velocity. Inset figure magnifies the linear slope in viscous sub-layer.

Blowing velocity (V_W) in wall normal direction is applied through the perforated surface from the perforated region as indicated with red color in Figure-1.3. V_W was varied in different magnitudes in a range $0 < V_W < 6\%$ of the free stream velocity for different experimental cases. This is expressed as BR, is a non dimensional parameter defined as the ratio between the blowing magnitude and the free stream velocity while expressed in percentage.

V_W is uniform in space, however, perforated surfaces must be used to approximate the ideal fully permeable surface for experimental realization. Therefore, by the term uniform blowing indicate uniformity of the blowing velocity in terms of the local spatial average. V_W is constant in space at least over the center of the holes, in addition, no intentional variation in space are present other than the ones that is accompanied by the use of a perforated area. Although this can not be strictly confirmed for the surface between the holes where blowing velocity is zero.

Figure-1.4 presents the outer scaled profiles of streamwise velocity along wall distance. The profiles were measured at the same streamwise location with different BRs where BRs were gradually doubled. Although other boundary conditions were same, the "dashed" line connecting the edge of the boundary visibly shows gradual increase of BLT with increasing BR, which supports the assumption stated in the previous section. The slope of the mean velocity near the wall is also presented in the inset figure, it also clearly observable that the wall shear is also decreased with increased BR.

Unlike canonical pipe flow, BLT of a turbulent boundary layer is ever increasing. Directly after the transition to turbulent regime, the growth of BLT is larger compared to the laminar one. One way to understand the mechanism of boundary layer growth is to consider the exchange of momentum. The exchange of fluid momentum in the vertical direction away from the plate is greater in turbulent boundary layer than that of the Laminar Boundary Layer. This is because the loss of momentum at the wall which is diffused either by viscosity (e.g. molecular mixing) or by turbulent mixing. An analytical solution of the turbulent boundary layer equations of motions are not possible unless otherwise numerically. It is rather more suitable to use the semi-empirical techniques in experiments.

Although drag reduction is however, of primary interest, for flow control experiments in wall bounded shear flows, many of the flow properties such as integral properties, mean and turbulence statistics, are also changed. Therefore, in addition to the BLT, other integral properties such as displacement thickness, momentum thickness and wall shear are changed as well. Beside integral properties, blowing also affects turbulence properties of the boundary layer. Statistics, particularly mean and Root-Mean-Square of all the velocity profiles are strongly affected and to be specific, blowing enhances them. However, these issues related to the effect of blowing on the turbulent boundary layer, we can summarize some of those as following research questions.

- How far in downstream direction does blowing influence the mean flow characteristics?
- Is coherence effected in the outer region with increasing blowing ratios?

- Is the change of the outer peak in RMS velocity profile a fundamental change in turbulence characteristics due to blowing? Do we observe changes to the existing coherent structures, particularly structures in the outer region, or do we observe complete new types?
- Turbulent structures in the outer layer influence the inner region structures, to understand how blowing affects this interaction is an important goal.
- What are the optimal parameters of blowing that will result in the formation of a second peak in power spectra and cross spectra in the outer region and how to interpret this second peak?
- How to determine the optimal geometric arrangement for perforated surface in order to achieve maximum influence on TBL control with minimum energy expense? Whether distribution of perforation and streamwise extent of blowing region effect the mean properties of the flow?
- How TKE and its fractional distribution is effected along the wall with different blowing ratio?
- Do we see different energy levels in spectrogram with different blowing ratios? For structures bigger than 2-3 δ, how does the distribution of spectral energy behave?
- Can we understand the physics of the reduction of wall shear stress and learn how to reduce friction drag by purpose of blowing application?

Turbulent boundary layer flows are of complex combination of different factors where the turbulent fluctuations are three dimensional which undergoes diffusion and transport of momentum. Energy of the turbulent structures present, have a continuous spectrum which are of self sustaining. There is a significant relationship between the production of Reynolds stress and these so-called turbulent structures. But blowing plays a strong role enhancing these Reynolds stresses and as a consequence, we expect significant modification to the frequency and energy aspect of these turbulent structures. In order to confirm such hypothesis, one has to look into the energy levels in spectrogram with different blowing ratios. Subsequently, how does the distribution of spectral energy behave.

Within the context of present thesis, we will deal primarily regarding the problems in canonical turbulent boundary layer associated with blowing such as scaling of blowing induced boundary layer, changes in their mean properties and turbulence statistics of the velocity profiles. One part of the present thesis deals with the inner scaling of the boundary layer profiles, friction parameters (wall shear velocity and friction coefficient) at moderate Reynolds number where as another part of the thesis discusses the turbulence statistics, their scaling, momentum transfer and Turbulent Kinetic Energy at high Reynolds number. Second part of this thesis also seeks to interpret the outer peak changes due to blowing. Blowing adds momentum flux into the flow, modify the diffusion process and enhances the Turbulent Kinetic Energy as a consequence.

Therefore, the region is investigated which is affected the most. In addition, we looked into the morphology of the coherent structures and investigated the effect of blowing.

As just said above, a TBL flow is very complicated and depends on many parameters and boundary conditions. The topic of such flow has been and still being investigated for centuries, many books are devoted wholly or in part to the theme of the turbulent flow. In a special series are the works of Rotta (1953), Tennekes (1972), Schlichting (1960), Pope (2000) and White (1974) where interested readers can find elaborate knowledge on the following topic.

1.4.1 Physics of a blowing induced Turbulent Boundary Layer

The boundary layer flow being investigated within the context of present thesis is assumed to be turbulent, incompressible e.g with constant viscosity and without heat transfer.

The continuity equation and simplified Navier-Stokes solution for incompressible, two-dimensional equation of motion representing the conservation of momentum and total shear stress for TBL under constant pressure is given below, where, the velocity components $\bar{u}(x,y)$, $\bar{v}(x,y)$ and P_∞ represents the time averaged streamwise and wall-normal components of the velocity, the pressure outside the boundary layer respectively. μ and ρ indicate the dynamic viscosity and density of air respectively. $u'(t,x,y)$, $v'(t,x,y)$ and $p'(t,x,y)$ are the fluctuating components.

$$\frac{\partial \bar{u}}{\partial x} + \frac{\partial \bar{v}}{\partial y} = 0 \qquad \text{(continuity)}$$

$$\bar{u}\frac{\partial \bar{u}}{\partial x} + \bar{v}\frac{\partial \bar{u}}{\partial y} = -\frac{1}{\rho}\frac{\partial P_\infty}{\partial x} + \frac{\mu}{\rho}\frac{\partial^2 \bar{u}}{\partial y^2} - \frac{\partial \overline{u'v'}}{\partial y}\frac{\partial}{\partial x}(\overline{u'^2} - \overline{v'^2}) \qquad \text{(Navier-Stokes)} \tag{1.1}$$

Reynolds decomposition of the corresponding velocity component are:

$$u = \bar{u} + u', \qquad v = \bar{v} + v' \tag{1.2}$$

Present thesis performed experiments on turbulent boundary layer over smooth surface in order to outline the reference characteristics. Therefore, boundary conditions at wall for reference turbulent boundary layer over an impermeable surface are defined with Equation-1.3.

$$\begin{aligned} &\bar{u} = 0 && \bar{v} = 0 && y = 0 \\ &\bar{u} = U_\infty && y = y \end{aligned} \tag{1.3}$$

As we are currently dealing with the zero pressure gradient, therefore, the first term in the R.H.S of Equation-1.1(Navier-Stokes) e.g $\partial P_\infty / \partial x = 0$. The fourth term in the same equation is of secondary importance and will be neglected thereafter. This term becomes

important as the flow reaches the point of separation, however, BRs used for the present experiment were selected as such that the flow never reached the point of separation. The second and the third component of the equation provides the wall normal variation of the total shear stress τ and is presented with the Equation-1.4. Integrating Equation-1.4 following this boundary condition, we obtain the expression for the total shear stress through Equation-1.5, where first and last term in the R.H.S present the *Viscous Shear Stress* (VSS) and *Reynolds Shear Stress* (RSS) respectively.

$$\frac{1}{\rho}\frac{\partial \tau}{\partial y} = \frac{\mu}{\rho}\frac{\partial \bar{u}}{\partial y} - \frac{\partial \overline{u'v'}}{\partial y} \tag{1.4}$$

$$\tau = \mu\frac{\partial \bar{u}}{\partial y} - \rho\overline{u'v'} \tag{1.5}$$

Further experiments were conducted over perforated surface with uniform blowing. In principle, boundary condition defined by Equation-1.3 has a modification when wall normal blowing at uniform rate is applied. Therefore, we can re-write Equation-1.3 as 1.6 which is the boundary condition under the influence of uniform blowing.

$$\begin{aligned} &\bar{u} = 0 && \bar{v} = V_W && y = 0 \\ &\bar{u} = U_\infty && y = y \end{aligned} \tag{1.6}$$

The influence of fluid viscosity creates the wall shear stress (τ_w) which extracts energy from the mean flow. The intermittent boundary between the potential flow and the boundary layer supply the energy required to feed into this wall shear stress.

$$\delta(x) \;=\; y(x, y), \bar{u} = 0.99U_\infty \tag{1.7}$$

This takes place at the edge of the boundary layer. A general description of this edge separating the non rotating potential flow is relevant which is described with the help of the BLT. This is presented in Equation-1.7.

It is known as the distance from the wall where the time averaged mean streamwise velocity reaches its 99%. Although, BLT of the turbulent boundary layer is presented with a mean value, in reality this is strongly intermittent in space and unsteady in time. Therefore, requires higher spatial resolutions with smaller velocity difference and subsequently, interpolation of the data points of the boundary layer velocity profile. Hence, uncertainty estimation is high for the statistical representation of the data. Figure-1.5 presents the BLT detection method visually using data obtained at $Re_\theta = 1870$.

It is often preferred to describe the turbulent boundary layer with the help of Integral properties of the turbulent boundary layer such as *displacement thickness* and *momentum thickness*. Such integral properties offer less error compared to the ones obtained from the interpolated values such as BLT. Pohlhausen (1921) derived a simplified method to calculate these integral parameters by solving Equation-1.1. The solution is also known popularly as momentum integral equation. Equation-1.8 presents the displacement thickness (δ^*).

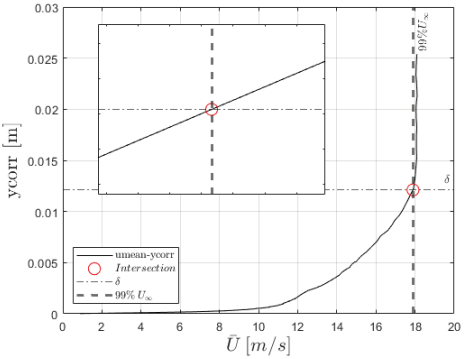

Figure 1.5: Dimensional streamwise velocity distribution along the wall distance using LDA method. Inset figure magnifies the region of interpolation with the $\bar{u} = 0.99U_\infty$.

Due to the frictional dissipation, the boundary layer can be considered to possess a total momentum flux deficit. This momentum loss in comparison to the potential flow is expressed as momentum thickness (θ) through Equation-1.9. The upper limit of the wall distance in Equation-1.8 and 1.9 is suggested to be set at the BLT. For determination of the integral length scales within the present thesis, we have set the outer limit of integration as the wall distance where mean streamwise velocity reaches 99%.

Rotta (1950) proposed a different length scale using the free stream velocity, wall shear velocity and the displacement thickness knows as Rotta-Clauser length scale (Δ) as expressed in Equation-1.10. The Rotta-Clauser length scale is also derived using an integral length scale e.g displacement thickness and therefore, easier to calculate from experimental data with relatively few number of data points along the boundary layer. Here, $u_\tau = \sqrt{(\tau_w(x)/\rho)}$. $\tau_W(x) = \mu(d\bar{u}/dy)$ is the local shear stress at wall which depends on the distance from the leading edge of the plate. Subsequently, we derive the skin friction coefficient by normalizing wall shear stress with the dynamic pressure of the free stream e.g $C_f = \tau_W/0.5\rho U_\infty^2$. In order to verify the experimental results, Smits et al. (1983) proposed an empirically derived power law for turbulent boundary layer flows over smooth wall and expressed as $C_f Re_{\theta,SBL} = K$, where constant $K = 0.024$.

$$\delta^* = \int_{y=0}^{\infty} (1 - \frac{\bar{u}}{U_\infty}) dy \tag{1.8}$$

$$\theta = \int_{y=0}^{\infty} \frac{\bar{u}}{U_\infty} (1 - \frac{\bar{u}}{U_\infty}) dy \tag{1.9}$$

$$\Delta = \frac{U_\infty \delta^*}{u_\tau} \tag{1.10}$$